Synthesis and Self-Assembly of Copolymers with Pendant Electroactive Units

Satyananda Barik and Suresh Valiyaveettil*

Department of Chemistry, 3-Science Drive 3, National University of Singapore, Singapore 117543, Singapore

Received April 14, 2008; Revised Manuscript Received June 8, 2008

ABSTRACT: The methacrylic copolymers incorporated with electroactive groups such as thiophene, carbazole, and fluorene moieties on the side chain were synthesized. Our approach consists of incorporating multiple electroactive functional groups onto a polymer backbone that can be used to develop functional materials. All copolymers were characterized, and a systematic structure−property relationship study was established. The structure and morphology of supramolecular self-assembly of copolymers were studied using transmission electron microscopy, wide-angle X-ray diffraction, and atomic force microscopy. Polymers can be patterned using an atomic force microscope, and nanosized lines or dots can be drawn on the polymer films. Polymer nanotubes obtained through self-assembly can be further stabilized by electropolymerization of the side chains.

Introduction

The self-assembly of copolymers into nanostructure aggregates has received considerable attention in research activity due to their ability to form different morphologies in bulk or in solution.[1−7] The potential of copolymers with incompatible units for nanotechnology has been realized in the past decade such as drug delivery,[2] nanomaterial synthesis,[3] nanolithography,[4] catalysis,[5] membrane separation,[6] dispersant technologies,[7] and molecular recognition.[8] Interesting architectures, such as spheres, rods, and vesicles, were formed through self-assembly of copolymers.[9] Among the different morphologies obtained from amphiphilic polymers include micelles and vesicles which are currently used in many applications.[10]

Polymer aggregates in the form of hollow spheres, lamella, and hollow cylinders were observed from the self-organization of rod−coil polymers depending on the solvent selected for the segments.[11] Self-assembly of copolymers into nanostructure aggregates reported to date include zero-,[12] one-,[13] and two-dimensional[14] assemblies based on the different thermodynamic/kinetic interactions like hydrogen bonding,[15] metal−ligand coordinate bonding,[16] aromatic $\pi-\pi$ interaction,[17] and hydrophobic effect.[18]

Self-organization of extended π-electron-rich molecules based on the programmed intermolecular noncovalent interactions is a powerful strategy in view of spontaneous and quantitative formation of well-defined nanoobjects.[19] In the case of polymers with aromatic moieties on the side chain, the main challenge in assembling large aromatic molecules into 1D structure lies in balancing the molecular assembly for growth along the π-stacking direction against the lateral association of polymer backbone or side chain alkyl units.[20] For a sample, triphenylene acrylate copolymer showed a hexagonal columnar mesophase. Similarly with dendron−rod−coil copolymer with dendron (aromatic) side chain units formed a ribbon-like morphology due to noncovalent interactions such as $\pi-\pi$ stacking and hydrogen bonding.[15−18] Advincula et al. have demonstrated viability of the "precursor polymer" approach based on single/binary pendant electroactive monomer groups (e.g., carbazole, thiophene) on the polymer backbone, which can be polymerized electrochemically for the device applications.[21] The composition of copolymer plays a significant influence on size, shape, and the stability of the supramolecular assemblies. A number of rod−coil copolymers of hole transporting unit (carbazole) or electron transporting unit (fluorene/thiophene) on the side chain have been reported for their unusual morphologies.[22]

In this report, we describe investigations designed to probe the supramolecular assembly of a few amphiphilic copolymers with interesting binary pendant electroactive side chains. We have incorporated a series of electropolymerizable groups on the polymer backbone and varied the length and nature (hydrophobic/hydrophilic) of the spacer groups (Figure 1). These designed copolymers have an inherent capacity to form fine structures in a few nanometers to micrometer scale. The electroactive units on the side chain can be electropolymerized in solution (cyclic voltammetry) and in thin films (AFM) followed by characterization with FT-IR investigation. The aggregation and electropolymerization (AFM/ CV) allow us to design materials with diverse and unique properties.

Experimental Section

Chemicals and Methods. All reactions were carried out under an inert atmosphere (N_2 or argon), unless specified. All reagents were purchased from commercial sources and used without further purification. All reactions were carried out with freshly distilled anhydrous solvents under an inert atmosphere. Tetrahydrofuran (THF) was purified by distillation over sodium under a nitrogen atmosphere. Carbazole and 2,2′-azoisobutyronitrile (AIBN) (Fluka) were purified using repeated recrystallization from methanol at room temperature.

The ^{1}H and ^{13}C NMR spectra were collected on a Bruker ACF 300 spectrometer operating at 300 and 75.5 MHz, respectively. Chloroform-*d* was used as solvent for NMR measurements with tetramethylsilane as internal standard. FT-IR spectra were recorded on a Bio-Rad FTS 165 spectrophotometer using KBr as matrix for solid and NaCl cell for liquid samples. The UV−vis spectra were recorded using a Shimadzu 3101 PC spectrophotometer, and fluorescence measurements were made on a RF-5301PC Shimadzu spectrophotometer in THF. Thermogravimetric analyses (TGA) were done using a TA Instruments SDT 2960 with a heating rate 10 °C/min under a nitrogen atmosphere. Differential scanning calorimetry (DSC) measurements were done on a TA Instruments DSC 2960 at a heating rate of 20 °C/min. Gel permeation chromatography (GPC) was used to obtain the molecular weight of the polymers with reference to polystyrene standards with THF as eluant. The morphology of the film was studied using transmission electron microscope (TEM), and the wide-angle X-ray scat-

* To whom correspondence should be addressed: Tel (65) 68744327, Fax (65) 67791691, e-mail chmsv@nus.edu.sg.

10.1021/ma8008349 CCC: $40.75
Published on Web 08/08/2008

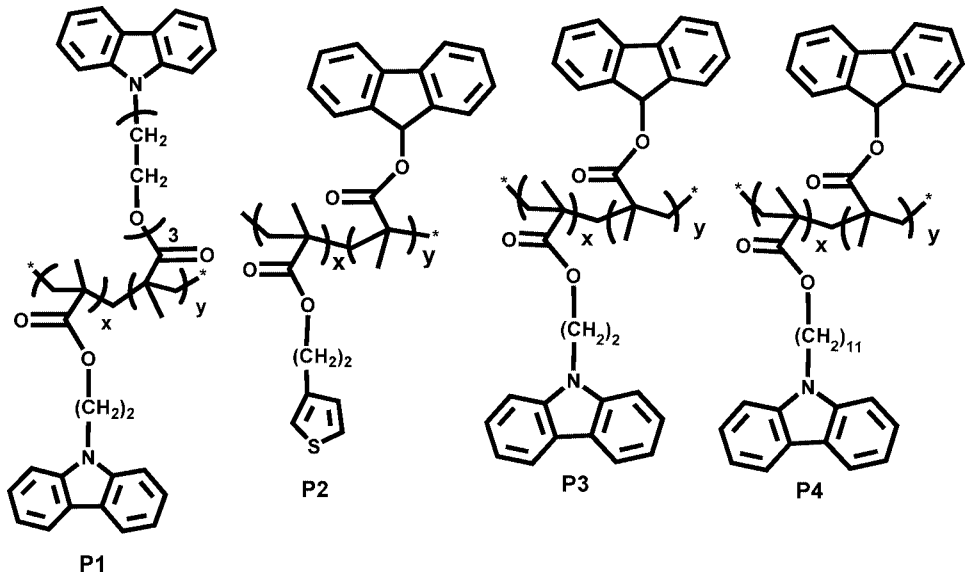

Figure 1. Molecular structures of copolymers **P1**−**P4**.

tering patterns were obtained using a D5005 Siemens X-ray diffractometer with Cu Kα (1.54 Å) radiation (40 kV, 40 mA). Samples were mounted on a sample holder and scanned between $2\theta = 2°$ and 50° with a step size of $2\theta = 0.01°$/min. A NanoMan AFM system with Au-coated Si_3N_4 contact tips was used for all nanopatterning experiments. *I*−*V* response measurements were performed on the nanopatterned area using conductive AFM (CAFM), in which a current sensor with a range of microamps to femtoamps was used. All polymers are soluble in common organic solvents such as THF, dichloromethane (DCM), and chloroform ($CHCl_3$).

Synthesis. The primary synthetic goal was to synthesize methacrylated monomers with electroactive units in the side chain. A few multicomponent copolymers with hydrophobic rigid aromatic units attached to the polymer backbone were designed and synthesized. Here, the monomers and polymers (**P1**−**P4**) were prepared using synthetic routes shown in Scheme 1 and Scheme 2.[23b−h] So the synthesis began with the reaction of inexpensive and commercially available starting materials with electroactive units like carbazole (**1**), 9-fluorenol (**8**), and thienylethanol (**10**) (Scheme 1). *N*-(2-Hydroxyethyl)carbazole (**2**) and 9-(11-hydroxyundecyl)carbazole (**4**) of carbazole derivatives were synthesized from carbazole.[23c,f] The corresponding methacrylated monomers **3**, **5**, **9**, and **11** was synthesized by esterification of hydroxy group containing electroactive units (**2**, **4**, **8**, and **10**) with methacryloyl chloride in THF and triethylamine at room temperature.[23c,g,h]The detailed synthesis and characterization of monomers is given in the Supporting Information.

Synthesis of 2-(2-Carbazol-9-yl-ethoxy)ethanol (6). Potassium hydroxide (6.0 g) was dissolved in DMSO (50 mL) and stirred for 1 h to get a clear solution. The mixture was stirred for another 1 h with carbazole (1) (4.0 g, 23 mmol) at room temperature followed by triethylbenzylammonium chloride (0.1 g) as phase transfer catalyst. 2-[2-(2-Chloroethoxyethoxy)]ethanol (4.44 g, 26 mmol) was added slowly and stirred for another 14 h. The mixture was poured into water (800 mL) and extracted with ether; the organic layer was dried over anhydrous Na_2SO_4 and filtered. The solvent was removed under reduced pressure, and the solid was purified by column chromatography using hexane/ethyl acetate (4:6 v/v) as eluent to gets low melting solid (yellow). Yield: 2.08 g (yield 33%). ^{1}H NMR ($CDCl_3$, δ, ppm): 8.07 (d, 2H, Cz), 7.45 (m, 4H, Cz), 7.25 (m, 2H, Cz), 4.51 (t, 2H, O−CH_2−CH_2−), 3.88 (t, 2H, N−CH_2−CH_2−), 0.86 (m, 6H, CH_2). ^{13}C NMR ($CDCl_3$, δ, ppm): 43.1, 61.8, 69.1, 69.3, 70.5, 71.0, 108.8, 119.0, 120.2, 122.9, 125.7, 136.1. EI-MS: 229.0 (M+). Elemental analysis: calcd C, 72.22; H, 7.07; N, 4.68; found: C, 72.21; H, 7.04; N, 4.72.

Synthesis of [2-(2-Carbazol-9-yl-ethoxy)ethyl] Methacrylate (7). A solution of **6** (2 g, 6.6 mmol) and triethylamine (1.0 g, 9.9 mmol) was dissolved in 80 mL of dry THF. The reaction mixture was cooled to 0 °C, and a solution of methacryloyl chloride (0.69 g, 6.6 mmol) in THF (20 mL) was added slowly to the reaction mixture. After the addition of methacryloyl chloride, the reaction mixture was stirred at room temperature overnight. Solvent was removed under high vacuum, and the residue was dissolved in a saturated solution of $NaHCO_3$. The product was extracted with ether, and the organic layer was washed with water three times (3 × 10 mL) and dried over Na_2SO_4. The solvent was removed under reduced pressure, and the solid was recrystallized from ethanol/chloroform (2:1) to yield 1.27 g (50%) of 3D. ^{1}H NMR ($CDCl_3$, δ, ppm): 8.06 (d, 2H, Cz), 7.43 (m, 4H, Cz), 7.23 (m, 2H, Cz), 6.08 (s, 1H, *trans*-vinylene), 5.52 (s, 1H, *cis*-vinylene), 4.46 (t, 2H, O−CH_2−CH_2−O), 4.16 (t, 2H, O−CH_2−CH_2−N), 3.81 (t, 2H, N−CH_2−CH_2−), 3.54 (t, 2H, CH_2), 1.91 (s, 3H, CH_3). ^{13}C NMR ($CDCl_3$, δ, ppm): 18.3, 43.1, 63.8, 69.1, 69.3, 70.59, 71.04, 108.8, 119.0, 120.2, 122.9, 125.6, 125.7, 136.1, 140.6, 167.3. EI-MS: 367.20 (M+). Elemental analysis: calcd C, 71.91; H, 6.86; N, 3.81; found: C, 71.92; H, 6.88; N, 3.82.

Synthesis and Characterization of Copolymers (Scheme 2). The synthetic scheme for copolymers **P1**−**P4** is shown in Scheme 2. The polymerizations of all methacrylate monomers for their homopolymer and copolymers were carried out using standard procedures reported in the literature.[23]

*General Procedure for Copolymerization (**P1**−**P4**).* The radical copolymerization of methacrylic monomers with pendant electroactive groups was carried out under a N_2 atmosphere. A solution of monomers in 20 mL of dry toluene was purged with N_2 for 30 min. The free radical initiator AIBN (5 mol % of total monomer concentration) was added and stirred under N_2 for another 30 min. The polymerization was started by heating the mixture at 60 °C for 2 days. The light yellow color reaction mixture was cooled to room temperature and precipitated in 300 mL of methanol with vigorous stirring. The resulting solid was collected by filtration and reprecipitated from hexane three times and dried under vacuum at 60 °C.

P1. Yellowish amorphous solid, yield 60%. ^{1}H NMR ($CDCl_3$, δ, ppm): 7.9 (b, 2H, Cz), 7.25 (m, 4H, Cz), 7.07 (b, 2H, Cz), 4.67 (b, 2H, O−CH_2), 4.2 (b, 2H, O−CH_2−CH_2−O), 3.55 (b, 2H, N−CH_2), 1.52 (b, 3H, CH_3). ^{13}C NMR ($CDCl_3$, δ ppm): 43.0, 69.2, 70.2, 70.7, 70.9, 108.8, 119.2, 120.2, 125.5, 125.7, 140.1, 140.4. FT-IR (KBr, cm^{-1}): 3458, 3052, 2922, 2858, 1728, 1631, 1487, 1328, 1253, 1149, 751, 721, 613, 557. Elemental analysis for

Scheme 1. General Synthetic Approach to Monomers[a]

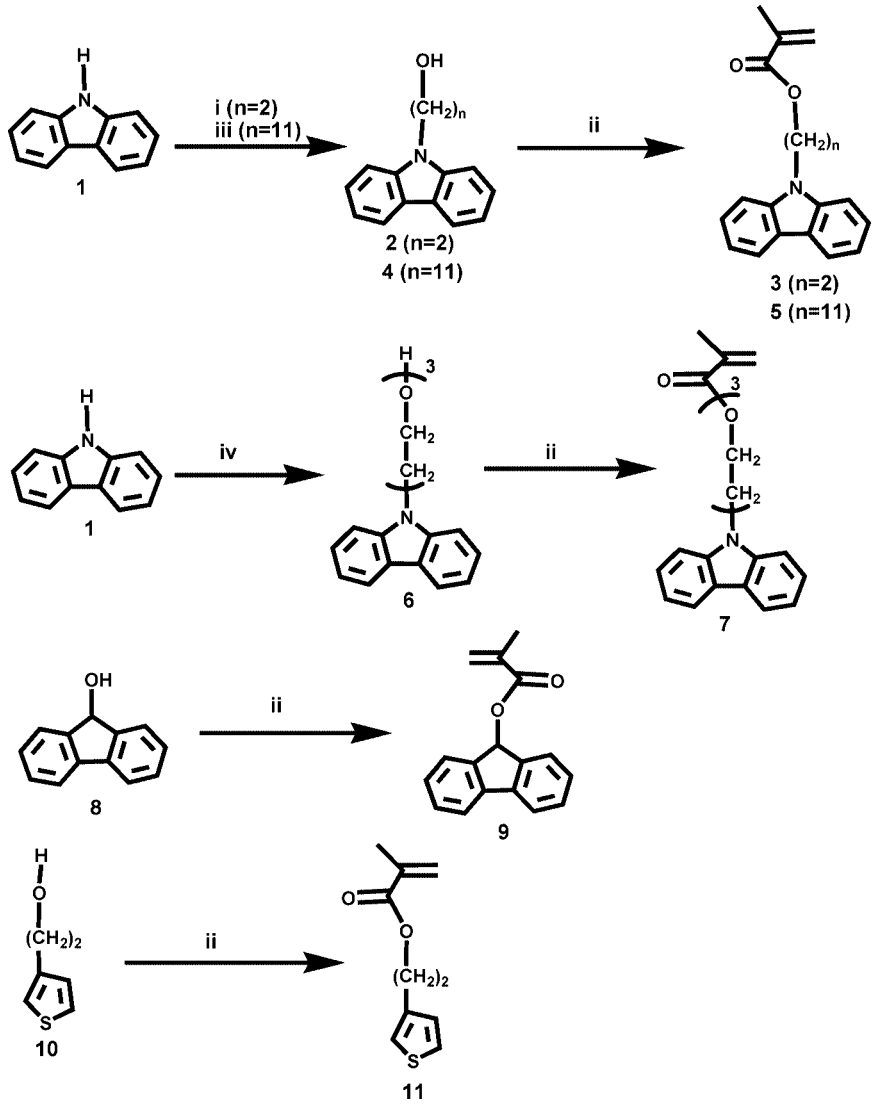

[a] Conditions: (i) 2-bromoethanol, KOH, DMSO, triethylbenzylammonium chloride, rt; (ii) triethylamine, THF, 0 °C; (iii) 11-bromo-1-undecanol, benzene, 50% NaOH, triethylbenzylammonium chloride, reflux 4 h; (iv) chloro(ethoxyethoxy)ethanol, DMSO, KOH, rt.

$(C_{39}H_{42}N_2O_6)_n$: calcd C, 73.77; H, 6.19; N, 4.53; found: C, 73.24; H, 6.19; N, 5.58.

P2. Gray amorphous solid, yield 65%. ^{1}H NMR ($CDCl_3$, δ, ppm): 7.57(b, 4H, Fl), 7.48−6.90 (m, 8H, Fl and Th), 6.46 (s, 1H, Fl), 4.32 (m, 2H, O−CH_2), 2.99 (m, 2H, O−CH_2−CH_2−), 2.10 (b, 6H, CH_3). ^{13}C NMR ($CDCl_3$, δ ppm): 22.6, 25.5, 29.0, 44.7, 67.9, 89.4, 119.8, 121.6, 125.7, 126.7, 127.6, 128.1, 129.5, 137.7, 137. 9, 141.0, 181.2, 190.3. FT-IR (KBr, cm^{-1}): 3443, 3103, 3067, 2948, 1726, 1450, 1586, 1147, 974, 758, 744. Elemental analysis for $(C_{27}H_{26}SO_4)_n$: calcd C, 72.62; H, 5.87; S, 7.28; O, 14.33; found: C, 72.43; H, 6.20; S, 7.35.

P3. White amorphous solid, yield 72%. ^{1}H NMR ($CDCl_3$, δ, ppm): 7.87 (b, 2H, Cz), 7.52 (b, 2H, Fl), 6.90−7.15 (m, 8H, Fl and Cz), 6.48 (s, 1H, Fl), 4.35 (m, 2H, O−CH_2), 3.72 (m, 2H, −N−CH_2), 1.57 (s, 6H, CH_3). ^{13}C NMR ($CDCl_3$, δ, ppm): 14.8, 45.4, 108.5, 119.1, 119.8, 120.3, 122.8, 125.6, 126.8, 127.6, 129.4, 140, 140, 180.8. FT-IR (KBr, cm^{-1}): 3441, 3061, 2986, 2929, 1727, 1602, 1557, 1455, 1147, 745. Elemental analysis for $(C_{35}H_{31}NO_4)_n$: calcd C, 79.33; H, 5.90; N, 2.67; found: C, 78.92; H, 5.87; N, 2.20.

P4. White amorphous solid, yield 67%. ^{1}H NMR ($CDCl_3$, δ, ppm): 7.98 (b, 2H, Cz), 7.09−7.43 (m,10H, Fl and Cz), 6.36 (s, 1H, Fl), 4.10 (b, 2H, −O−CH_2), 3.79 (b, 2H, −N−CH_2), 2.05 (b, 6H, CH_3), 0.86−1.89 (m, 16H). ^{13}C NMR ($CDCl_3$, δ,ppm): 27.2, 28.8, 29.3, 42.9, 108.5, 118.5, 120.2, 122.7, 125.4, 140.3, 141. FT-IR (KBr, cm^{-1}): 3445, 3061, 2927, 2852, 1726, 1624, 1455, 1328, 1149, 973, 746. Elemental analysis for $(C_{44}H_{53}NO_4)_n$: calcd C, 79.37; H, 5.90; N, 2.64; found: C, 79.02; H, 7.12; N, 1.66.

Results and Discussion

Design and Synthesis of Monomers and Polymers. Bulky aromatic side chains were incorporated along the polymer backbone to control the aggregation and morphology in the polymer lattice through π-stacking. The target polymer structures involve a relatively flexible polymethacrylate chain and rigid electroactive pendant aromatic units in the side chain, which can be polymerized electrochemically (Figure 1). We chose groups such as carbazole, thiophene, and fluorene as side chains because of their potential applications as hole/electron transport materials in optoelectronic material. The length and flexibility of the spacer between the side chain and polymer backbone play an important role in controlling the self-assembly inside the polymer lattice.

The syntheses of monomers (Scheme 1) and copolymers (**P1**−**P4**) (Scheme 2) were achieved using a free radical polymerization method with AIBN as an initiator.[23]This technique afforded copolymers **P1**−**P4**, with good polydispersity

Scheme 2. General Synthetic Approach to Copolymers P1−P4[a]

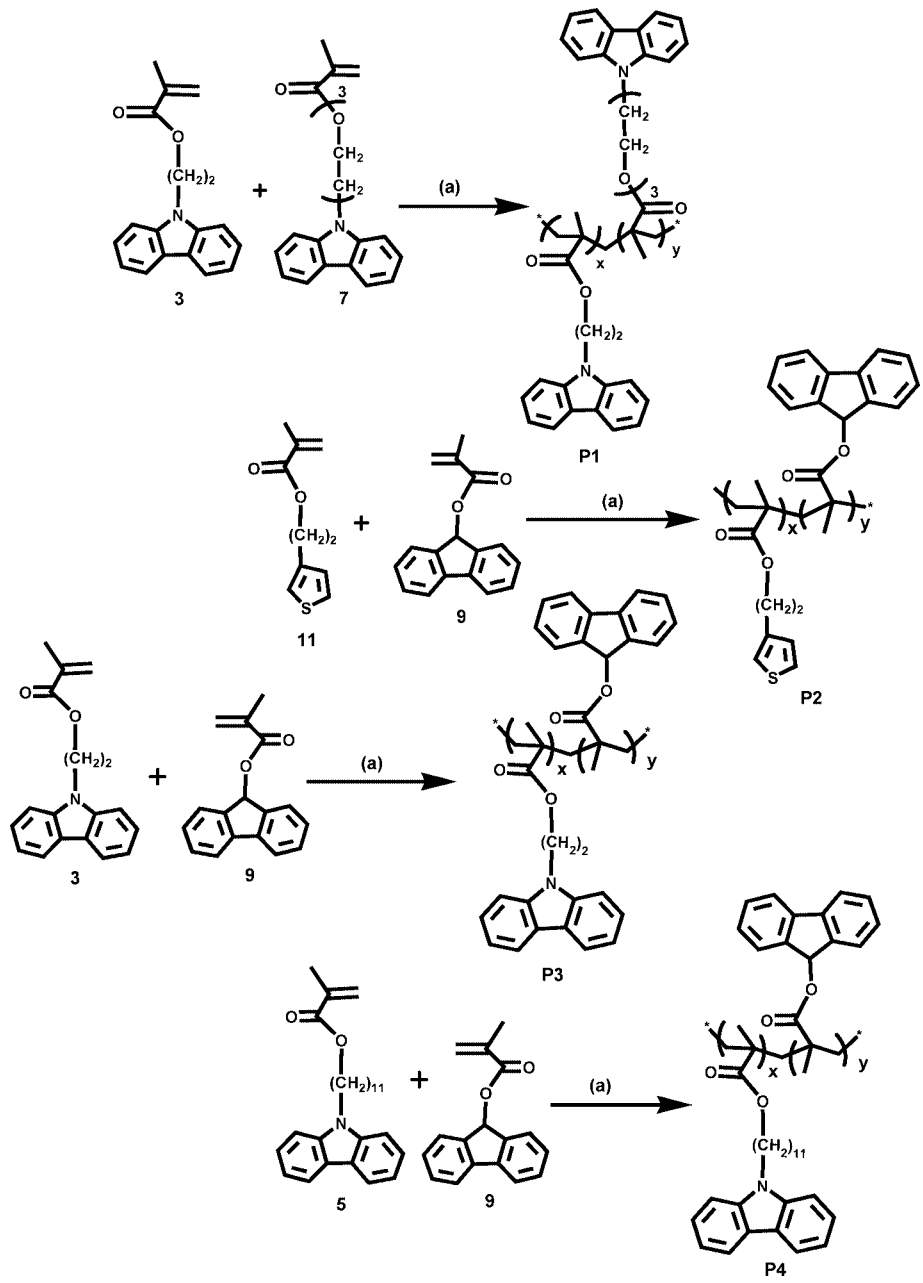

[a] Conditions: (a) toluene, AIBN (5 mol % of total monomer concentration), 60 °C, 2 days.

Table 1. Structural Characteristics of Polymers P1−P4

	molecular weight			thermal analysis	
copolymer	M_n	M_w	PD	T_d (°C)	T_g (°C)
P1	6 496	10 535	1.62	250	84
P2	20 200	32 000	1.67	207	116
P3	6 692	10 567	1.57	225	89
P4	16 874	28 076	1.66	253	82

(PD) and molecular weight (Table 1). All copolymers (**P1−P4**) were characterized using FT-IR, ^{1}H NMR, ^{13}C NMR, GPC, elemental analysis, TGA, and X-ray diffraction. As spacer length increases, the peaks in the NMR spectra become sharper and multiplets were better resolved.[16] The physical properties of copolymers **P1−P4** are listed in Table 1. The molecular weights of the polymers were measured by means of gel permeation chromatography (GPC) using THF as eluant and polystyrene as the standard (Table 1). All copolymers were soluble in common organic solvents such as THF, chloroform, dichlo-

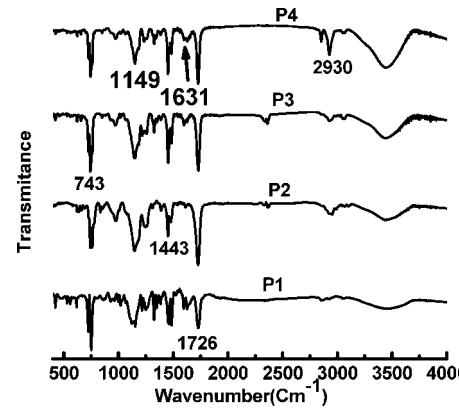

Figure 2. FT-IR spectra of copolymers **P1−P4**.

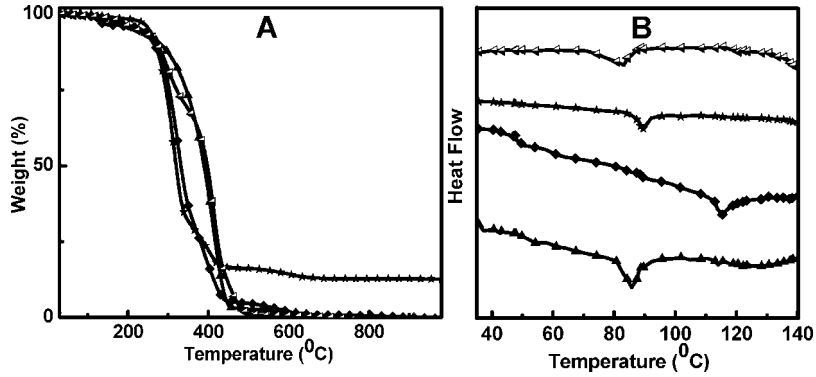

Figure 3. TGA (A) and DSC (B) of copolymers (▲) **P1**, (◆) **P2**, (★) **P3**, and (△) **P4** at heating rate of 10 °C/min under a N_2 atmosphere.

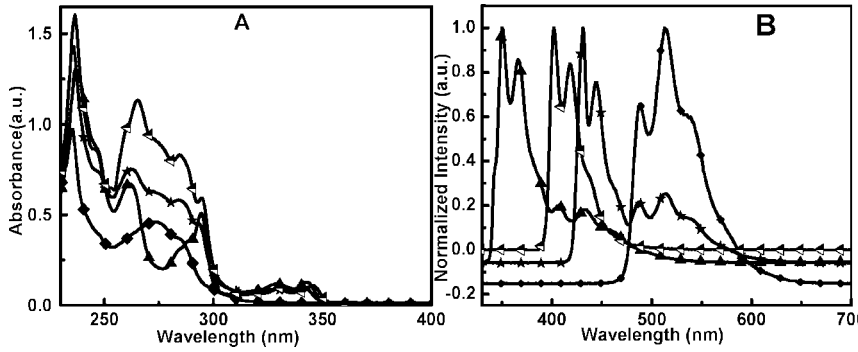

Figure 4. Absorption (A) and fluorescence spectra (B) of copolymers in THF solution: (▲) **P1**; (◆) **P2**; (★) **P3**; (△) **P4**.

Table 2. Absorption and Emission Wavelengths for Copolymers P1−P4 in THF

	solution (THF)		position of new absorption peaks appeared after electropolymerization of a thin film
copolymer	λ_{max} (nm)	λ_{ems} (nm)	λ_{max} (nm)
P1	266, 294, 330, 343	350, 366	301, 535
P2	236, 274	488, 513, 520	329, 545
P3	236, 266, 294, 330, 344	432, 444	301,349,440
P4	266, 294, 330, 344	402, 420	229,348,455

romethane, chlorobenzene, and toluene. The FT-IR spectra of the copolymers are given in Figure 2. The copolymers **P1**, **P3**, and **P4** containing a carbazole ring shows strong carbonyl band ($\nu \sim 1726$ cm^{-1}) and the corresponding ester linkage ($\nu \sim 1631$ cm^{-1}), −N−CH_2− bands for carbazole groups, and aromatic C−N stretching at $\nu \sim 1253$ cm^{-1}.

Thermal Properties. Thermal properties of the polymers were investigated using thermogravimetric analysis (TGA) and differential scanning calorimetry at a heating rate 10 °C/min under a nitrogen atmosphere (Figure 3). The thermograms indicated that the copolymers **P1**−**P4** are thermally stable up to 250 °C. The first onset degradation temperatures were in the range of 200−250 °C (Figure 3A). The glass transition temperatures of these copolymers ranged from 82 to 116 °C (Figure 3B). As expected, an increase in the spacer length and a decrease in T_g of the copolymer were observed owing to the increase in flexibility of the polymer. The copolymer **P2**, with no spacer, showed a maximum T_g (116 °C), whereas **P4** with C11-spacer linkage showed the lowest T_g (82 °C).

Optical Properties. *Absorption and Emission Spectra.* The representative absorption and emission spectra of copolymers in THF are shown in parts A and B of Figure 4, respectively. The copolymers do not exhibit any new bands other than the corresponding chromophore in the absorption spectra, indicating that there is no interaction between the chromophores in their ground state. For comparison, the UV−vis spectra of copolymers and corresponding homopolymers are shown in Figure S4 (Supporting Information). The spectrum of **P1**, which contains only carbazole unit, exhibited four strong absorption peaks at 266, 294, 330, and 343 nm, and the relevant carbazole homopolymers showed peaks at 260, 294, 330, and 344 nm with significant overlap. The absorption band at 294 nm corresponds to the S_0-S_1 transition of carbazole[17] units with a shoulder at 330 nm. The absorption and emission wavelengths for the copolymers **P1**−**P4** in THF are summarized in Table 2. **P2**, which contains fluorene and thiophene chromophores on the backbone, showed two strong absorptions at 240 and 275 nm, as compared to the thiophene and fluorene pendant methacylated homopolymers **HP4** (240 nm) and **HP2** (270 nm), respectively. The copolymers **P3** and **P4** containing fluorene and carbazole pendant units showed five absorption peaks at 260, 270, 294, 330, and 344 nm, whereas, the corresponding homopolymers showed similar peaks for each chromophores (see Supporting Information, Figure S4).

It is expected that the interactions between the neighboring chromophores along a polymer chain induce fluorescence quenching through various mechanisms.[23a] The fluorescence spectra of **P1**−**P4** in THF are shown in Figure 4B with the excitation wavelength corresponding to the maximum absorption wavelength. These compounds do not exhibit emission properties similar to that of the homopolymers. Fluorescence intensity of the homopolymers was lower than the corresponding copolymers at same chromophore concentration. The **P1** containing only carbazole units showed emission maxima at 353 and 366 nm. By introducing other chromophores on the polymer backbone, the emission and electrochemical properties can be significantly influenced.

Incorporation of fluorene and thiophene groups on the polymer backbone caused a red shift in the absorption maxima of the copolymer. Emission spectra of copolymers and homopolymers are given in Figure S4 in the Supporting Informa-

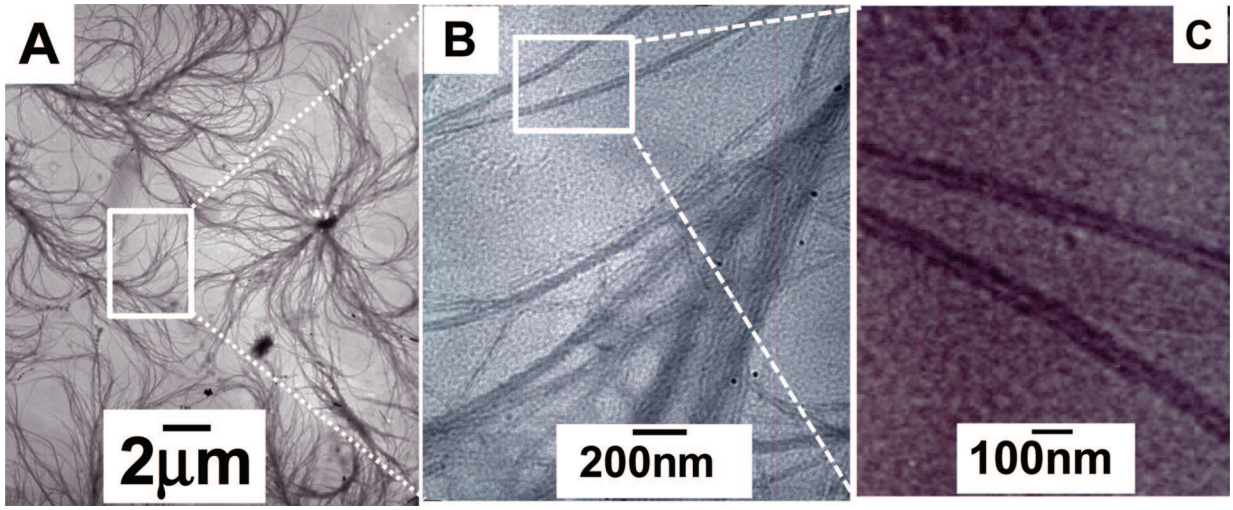

Figure 5. TEM images of nanofibers formed by self-assembly of copolymer **P2** at 0.01 mg/mL.

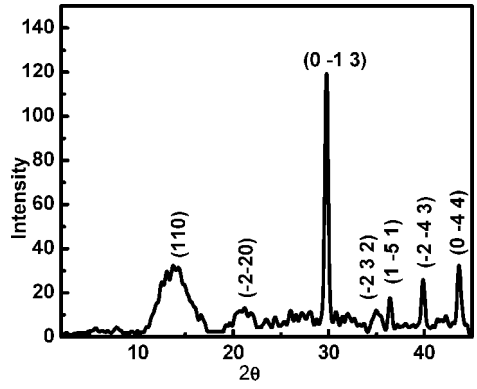

Figure 6. X-ray diffraction pattern of the copolymer **P2** film on a glass slide.

Table 3. X-ray Diffraction Data for Copolymer P2

diffraction angle (2θ) (deg)	*hkl*[a]	D_{obs} (Å)	d_{calc} (Å)	thickness of crystallites[b] (nm)
13.83	(110)	6.65	6.41	2.1
21.21	($\bar{2}$20)	4.18	4.18	3.6
29.76	(0$\bar{1}$3)	2.98	3.0	11.0
34.97	($\bar{2}$32)	2.56	2.56	7.0
36.35	(1$\bar{5}$1)	2.47	2.47	11.5
39.89	($\bar{2}\bar{4}$3)	2.25	2.25	11.5
43.63	(0$\bar{4}\bar{4}$)	2.07	2.07	11.5

[a] Deduced from International Centre for Diffraction Data 2006 (JCPDF Data). [b] Calculated from Scherrer's equation.[26b]

tion. The red shift in the emission maxima observed for all copolymers from their corresponding homopolymers indicates possible interaction between the substituents and change in conformation of the polymer backbone.

Characterization of the Nanofibers. The polymers **P1**−**P4** would be capable of forming solvent-dependent supramolecular self-assembly. Transmission electron microscopy (TEM) has been an effective tool for characterizing supramolecular self-assembly at nanometer dimensions.[24−26] For this purpose, the polymers were dissolved in different solvents such as THF, DCM, and $CHCl_3$ at a concentration of 0.01 mg/mL. A thin film was obtained on TEM grid through drop-casting of the solution. The TEM images obtained from the THF solution of the copolymer **P2** are shown in Figure 5, which suggests that **P2** forms hollow tubes 10−12 nm in diameter (Figure 5). In Figure 5A, tubes were seen with a focal point. The formation of one-dimensional (1D) hollow tubes could be explained using polymer chain aggregation through $\pi-\pi$ stacking of side chain units. All the copolymers formed nanofibers from THF solutions were fully characterized.

The formation of hollow elongated nanofibrils is expected to be due to a particular molecular ordering, which can be characterized using X-ray diffraction. Figure 6 shows the wide-angle X-ray diffraction pattern of the dried polymer film on a glass substrate. The sharp diffraction patterns (Table 3) indicate a highly crystalline nature of the polymer in solid state.

The nanofibers were formed by the self-assembly of polymers via $\pi-\pi$ interaction and hydrophobic interactions among the polymer chains. The *d*-spacings (calculated using Bragg's law) correspond to the $\pi-\pi$ interaction inferred from the sharp peak at 3.0 Å (2θ = 29.8°), which is close to the typical distance (~3.5 Å) for an effective $\pi-\pi$ stacking between the aromatic molecules.[26] Considering the hydrophobic interaction between the polymer chains, the broad peak with *d*-spacing of 6.41 Å (2θ = 13.83°) might be due to close packing of long alkyl chains. The breadth of the diffraction peaks can be used to measure thickness of crystallites using the Scherrer equation[26b] (Table 3). From the Scherrer equation, the thickness of the 2D crystallite calculated is similar to the thickness calculated from analysis of TEM micrographs (Figure 5). The expected conformation of the polymer chains in the nanofibers can be depicted as shown in Figure 7.

Electrochemical Nanopatterning of Polymer Film Using AFM. The patterning ability of all polymers was studied using AFM-assisted electrostatic lithography,[27] and the change in conductivity after cross-linking of the side-chain chromophores was explored using the conductive atomic force microscope (C-AFM) technique. In order to do the nanopatterning, polymer film was prepared by spin-coating a solution of copolymers in chlorobenzene (0.5 wt %) on a Si (100) substrate at 4000 rpm. The film was then annealed for 2 h at 100 °C, and the thickness of the film was measured as 98 nm using AFM. Various nanostructures were created on a polymer film via patterning at different applied bias and tip speed. Figure 8a shows that the AFM image of the line patterning on the polymer **P3** film with various tip bias of −7, −8, −9, −10, and −11 V at a tip speed of 0.5 μm/s. Here, the width of the nanopattern was increased with the increase of applied bias, and the pattern width extended rapidly at higher voltages of −10 and −11 V. Also, nanolines were drawn at various tip speeds of 1.0, 0.5, 0.1, and 0.05 μm/s at a tip bias of −9 V (Figure 8b). The broadening of pattern at higher voltage and a slow tip speed demonstrated easy patternability of the polymer films due to the presence of electroactive groups on the polymer backbone. Micrographs c

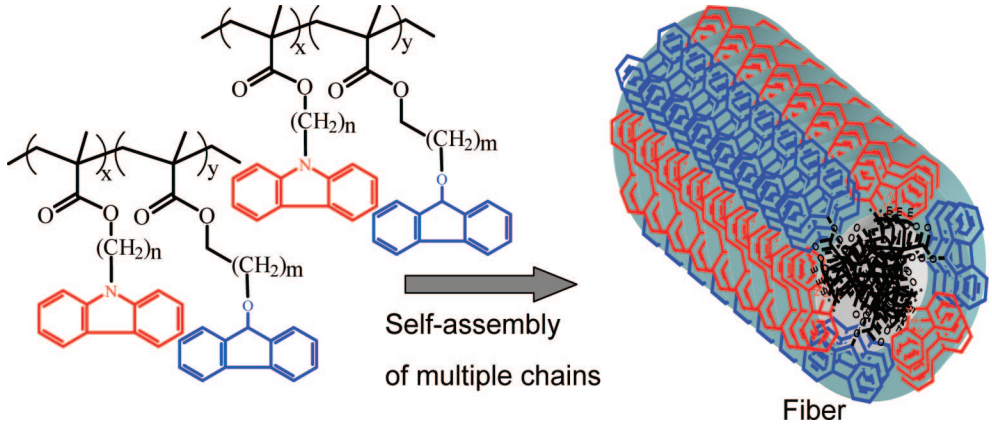

Figure 7. Schematic representation of molecular self-assembly through aggregation of polymer chains and $\pi-\pi$ stacking of the electroactive groups on the side chain.

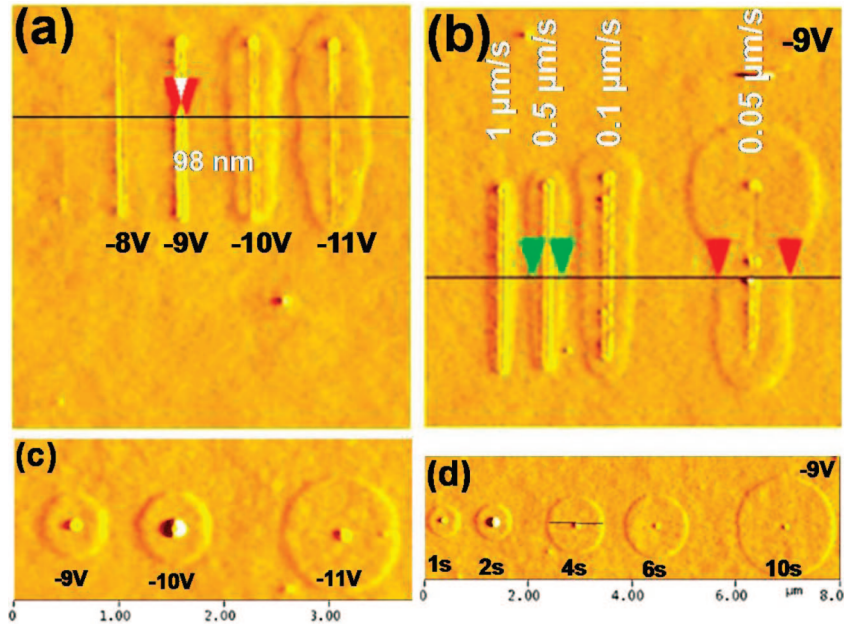

Figure 8. Nanopatterning of polymer **P3** film at various tip bias (a) and tip speed (b). Dot patterning on polymer film at various tip bias (c) and contact time (d).

and d of Figure 8 shows the dot patterning on the polymer film at various tip bias with contact time of 2 s and at different time intervals at a constant voltage of −9 V, respectively.

It is expected that cross-links can be formed between the electroactive monomer units on the side chain during the patterning. The conductivity of these nanopatterns formed through electrochemical process is measured using C-AFM, where the patterned region showed a higher conductivity than the unpatterned region. The cross-linked networks were formed by oxidation of electropolymerizable groups, such as carbazole/carbazole−fluorene/fluorene−thiophene rings on the polymer backbone.[28] Such electropolymerization can also be monitored using cyclic voltammetry (CV).

Electrochemical Polymerization. The polymers were electropolymerized using cyclic voltammetry in a three-electrode cell. The cell was equipped with Ag/AgCl/3.8 M KCl as a reference electrode and platinum as a counter electrode. The ITO was used as working electrode and the substrate. In the three cell compartments, 0.1 M tetrabutylammonium hexafluorophosphate (TBAP) was used as supporting electrolyte. The carbazole/fluorene/thiophene incorporated precursor polymers, **P1**−**P4** were spin-coated onto the ITO substrate and used for the experiment. Cyclic voltamograms of the polymer **(P1**−**P4)** films on ITO substrate with a scan rate of 50 mV/s are given in Figure 9. The oxidation onset for spin-coated polymer film of **P1** is 0.77 V, and the corresponding reduction peak is 0.43 V (Figure 9A), which are similar to the reported values for electropolymerization of carbazole.[29] The current increases gradually for the subsequent cycles.

For **P3** and **P4** (Figure 9C,D), two anodic oxidation peaks (Epa1 and Epa2) were observed in the range of 1.1−1.45 V with their corresponding reduction peaks (Epc1 and Epc2) potentials in the range of 0.78−1.18 V, after 10 cycles. It is interesting that after 5 cycles the Epc1 value did not increase but the Epc2 value constantly increased, suggesting the formation of polyfuorene (oxidation potential of fluorene is 1.25 V).[29h] Since the statistical ratio of carbazole to fluorene unit in the precursor polymer is 1:1, the formation of copolymer with carbazole−fluorene repeating units is expected after electropolymerization. On the basis of electron density, intermolecular coupling involving 2,7-positions predominate over 3,6-positions in the fluorene unit.[30] Similarly, the 3,6-position is expected to predominate over 2,7-positions of the carbazole units. In the same manner, copolymerization of thiophene and fluorene units on **P2** was achieved (Figure 9B). In case of **P2**, oxidation peaks were absent in the first cycle, but two oxidation peaks (Epa1

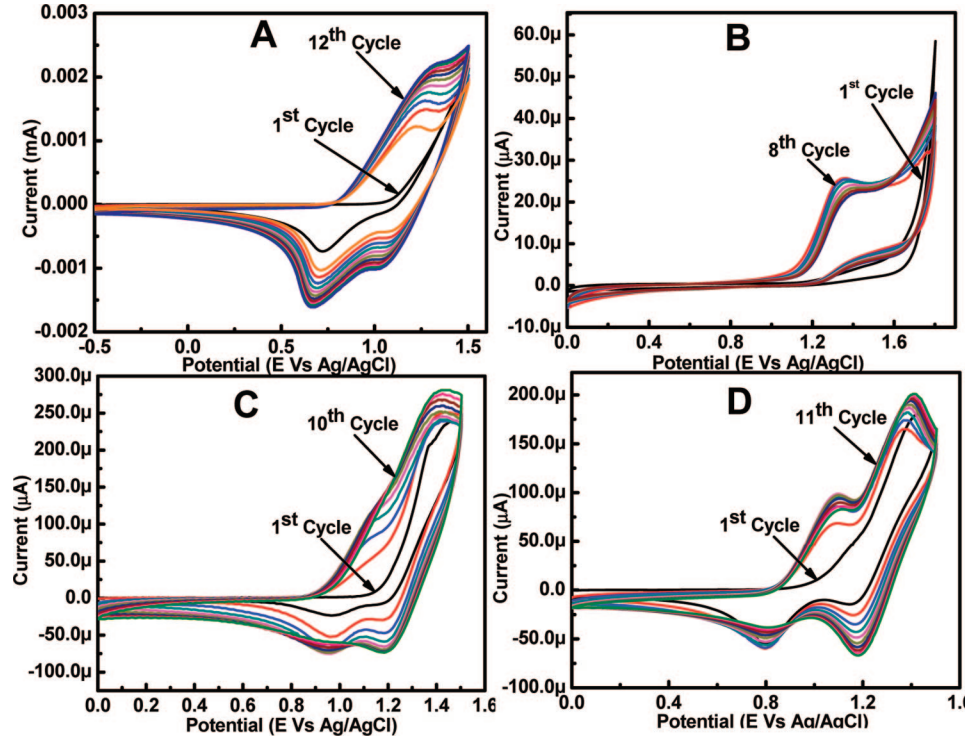

Figure 9. CV for electrochemical polymerization (cross-linking) of spin-coated polymer film in ITO substrate (A) **P1**, (B) **P2**, (C) **P3**, and (D) **P4** at the scan rate 50 mV/s.

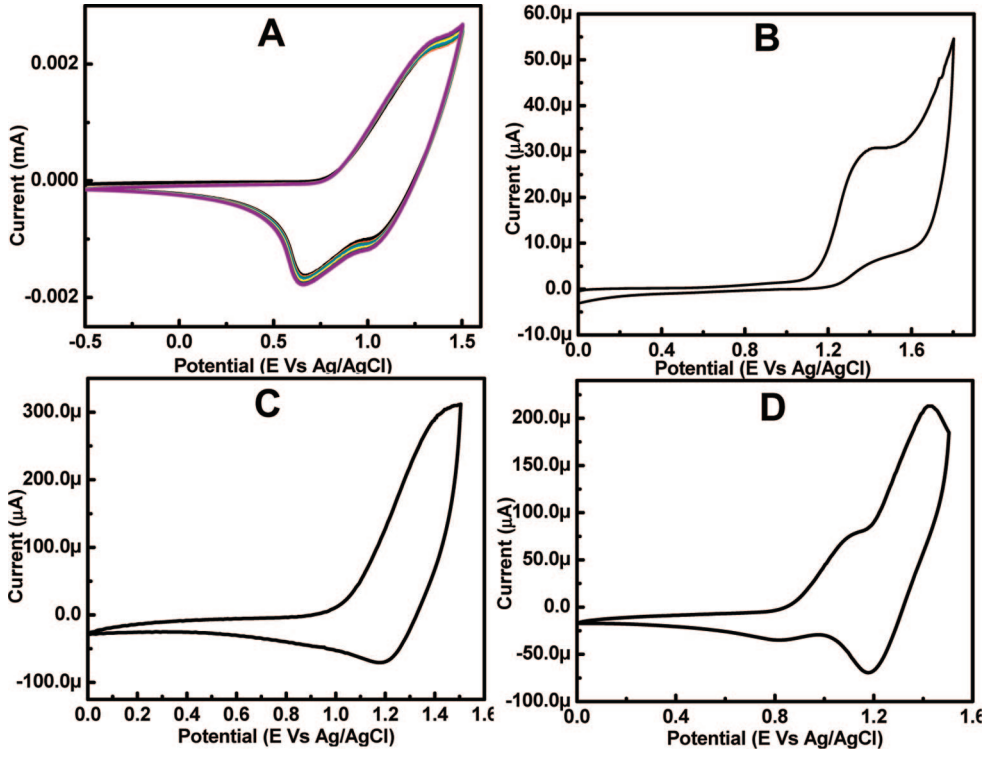

Figure 10. CV for polymer free scans of electrochemical cross-linking polymer films (A) **P1**, (B) **P2**, (C) **P3**, and (D) **P4**.

and Epa2) at 1.34 V and 1.75 V with corresponding reduction peaks (Epc1 and Epc2) at 1.25 and 1.61 V, respectively, appeared during repeated scans, which indicates that first cycle is different from the second cycle with the possibility of the cross-linking. A precursor polymer free scan using the already cross-linked polymer was performed and showed a characteristic oxidation and reduction peaks (Figure 10 A−D), with no further changes in the peak position or intensity during additional scans. This also indicated complete electropolymerization of all accessible side chains.

The electropolymerized thin films on ITO substrate were further characterized by UV−vis and FT-IR spectroscopic investigations. In the absorption spectra, a new broad band appeared at a long wavelength region after electropolymerization (Supporting Information, Figure S5). For copolymer **P1** with carbazole units, an absorption peak at 301 nm and a shoulder

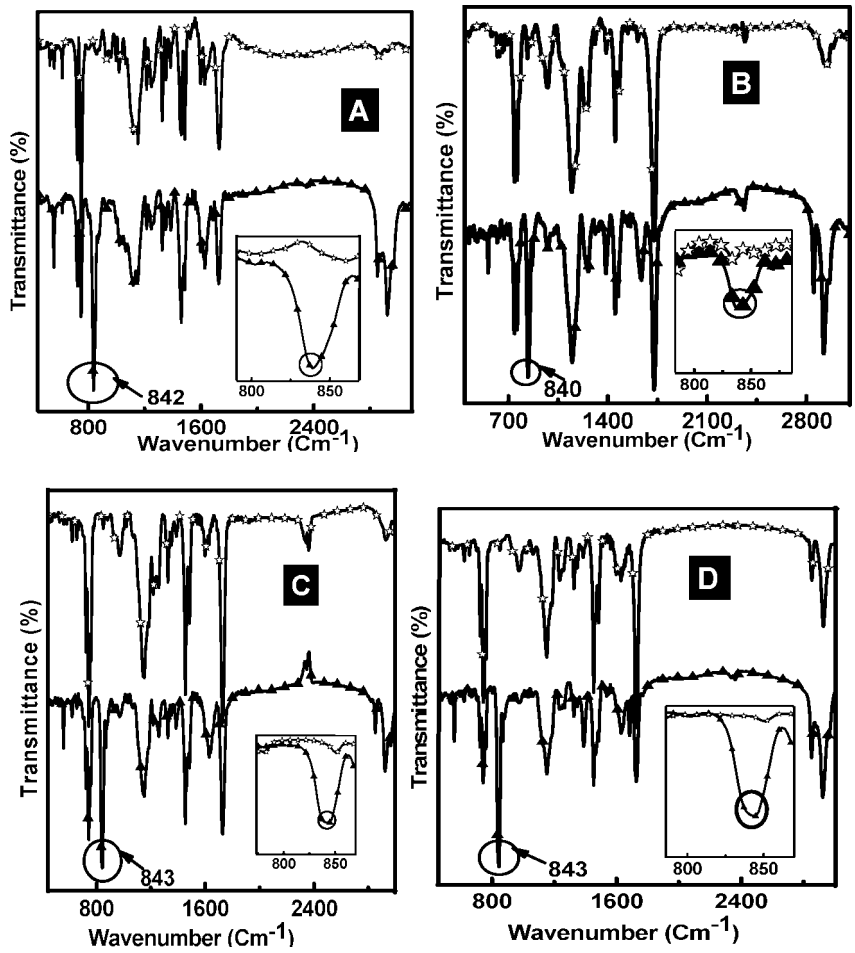

Figure 11. FT-IR spectra of electrochemical cross-linking polymer film with precursor polymers (A) **P1**, (B) **P2**, (C) **P3**, and (D) **P4**: (☆) precursor polymer; (▲) after electropolymerization. The characteristic peak which appeared after electropolymerization is shown in the inset.

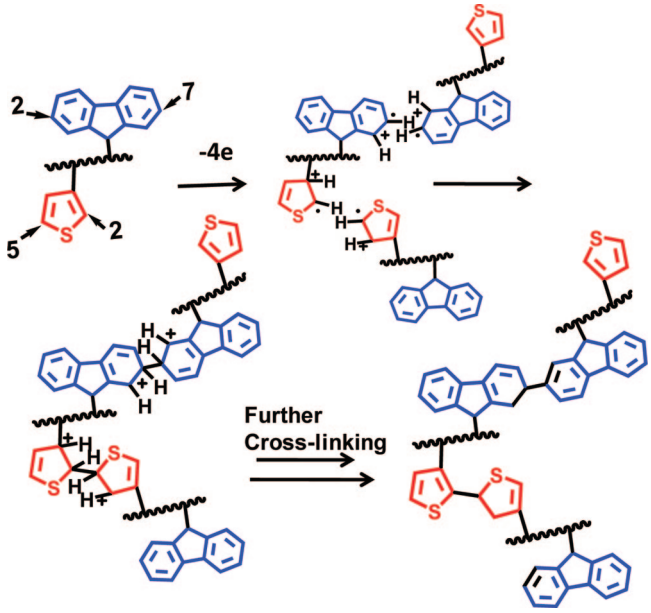

Figure 12. Mechanism for the electropolymerization (cationic) and cross-linking of **P2**.

at 345 nm were observed, which could be attributed due to the $\pi-\pi^*$ transition in polycarbazole.[32a] A broad peak around 535 nm appeared to be due to the formation of highly cross-linked copolymer. In case of **P2**, the observed red shift of absorption peaks at 301 and 330 nm indicated a high degree of cross-linked conjugated moieties on the polymer. The new peak at 555 nm is also attributed to the formation of fluorene and thiophene oligomers inside the polymer lattice.[32c,d]

Similarly, in case of **P3** and **P4**, the peak due to the $\pi-\pi^*$ transition appeared at 301 nm. The new peak which appeared around 455 nm is attributed to the polymerization of carbazole and fluorene. The absence of an absorption peak at 540 nm indicates that the individual carbazole polaronic transition is not seen from the cross-linked carbazole units.[32b−f] The UV−vis absorption spectra of the cross-linked polymer film are given in the Supporting Information in Figure S5.

The FT-IR spectra of **P1**−**P4** after electropolymrization are shown in Figure 11A−D. Comparing with the four precursor copolymers, the electropolymerized polymers showed cross-linking because of the appearance of extra peaks in the FT-IR spectrum at 840 cm^{-1}. The sharp peaks are due to the C−H out-of-plane bending vibrations of 1,2,3,4-substituted aromatic units.[31]

A schematic representation of the mechanism of cross-linking through electropolymerization is shown in Figure 12,[27b−e] in which the anodic oxidation leads to the formation of radical cations generated through the electroactive moieties. It appears that electron-rich substituents on the polymer backbone help to electropolymerize the side chains to form a polymer network. Work is in progress in our laboratory to find the degree of polymerization and conformation of the electropolymerized chains inside the polymer lattice.

Conclusion

A series of methacrylate-based copolymers containing aromatic electroactive units were prepared using free radical polymerization and investigated the cross-linking through electropolymerization. For all copolymers, glass transition temperature decreased with increasing the spacer length between the rigid aromatic units. The optical properties of the polymers showed little electronic interactions between the chromophore groups in solution or in thin films. The nanotubes of copolymers obtained from solution through self-assembly were fully characterized. The precursor polymers were electropolymerized using cyclic voltammetry (CV) and AFM. The anodic electropolymerization of precursor polymer film was confirmed through the C−C linkage in the FT-IR spectra, changes in absorption maxima, and increase in conductivity of the polymerized regions. The variation of polymer nanopatterning features with respect to the applied bias and tip speed was investigated. Electropolymerization and cross-linking ability of the electroactive precursor polymers (**P1**−**P4**) can be used for design and fabrication of potential devices.

Acknowledgment. We are grateful to Agency for Science, Technology and Research for funding support and Department of Chemistry and National University of Singapore Nanoscience and Nanotechnology Initiative (NUSNNI) for technical support. S.B. thanks the Ministry of Education for a scholarship through National University of Singapore.

Supporting Information Available: ^{1}H and ^{13}C NMR spectra of the copolymers (**P1**−**P4**), comparison of optical properties of copolymers with corresponding homopolymers, and the powder X-ray diffraction patterning of copolymers. This material is available free of charge via the Internet at http://pubs.acs.org.

References and Notes

(1) (a) Hamley, I. W. *Development in Block Copolymers Science and Technology*; Wiley & Sons: New York. (b) Patil, A. O.; Schulz, D. N.; Novak, B. M. *Functional Polymers: Modern Synthetic Methods and Novel Structures*; ACS Symposium Series 704; American Chemical Society: Washington, DC, 1997. (c) Hadjichristidis, N.; Pispas, S.; Floudas, G. *Block Copolymers: Synthetic Strategies, Physical Properties, and Application*; Wiley & Sons: New York, 2003.

(2) (a) Nishiyama, N.; Kataoka, K. *Adv. Polym. Sci.* **2006**, *193*, 67–101. (b) Allen, D.; Maysinger, D.; Eisenberg, A. *Colloids Surf., B* **1999**, *16*, 3–27.

(3) (a) Forster, S.; Antinietti, M. *Adv. Mater.* **1998**, *10*, 195–217. (b) Lazzari, M.; Lopez-Quintela, M. A. *Adv. Mater.* **2003**, *15*, 1583–1594. (c) Hamley, I. W. *Nanotechnology* **2003**, *14*, R39–54.

(4) (a) Jegadesan, S.; Advincula, R. C.; Valiyaveettil, S. *Adv. Mater.* **2005**, *17*, 1282–1285. (b) BucknallDavidD. G. *Nanolithography and patterening Techniques in Microelectronics*; CRC Press: Boca Raton, FL, 2005.

(5) (a) Rossbach, B. M.; Leopold, K.; Weberskirch, R. *Angew. Chem., Int. Ed.* **2006**, *45*, 1309–1312. (b) Durkee, D. A.; Eitouni, H. B.; Gomez, E. D.; Ellsworth, M. W.; Bell, A. T.; Balsara, N. P. *Adv. Mater.* **2005**, *17*, 2003–2006.

(6) (a) Sperschneider, A.; Schacher, F.; Marcel, G.; Tsarkova, L.; Muller, A. H.E. *Small* **2007**, *3*, 1056–1063. (b) Choucair, A.; Eisenberg, A. *J. Am. Chem. Soc.* **2003**, *125*, 11993–12000.

(7) (a) Liu, G.; Yang, H.; Zhou, J.; Law, S. J.; Jiang, Q.; Yang, G. *Biomacromolecules* **2005**, *6*, 1280–1288. (b) Shin, H. I.; Min, B. G.; Jeong, W.; Park, C. *Macromol. Rapid Commun.* **2005**, *26*, 1451–1457. (c) Moad, G.; Dean, K.; Edmond, L.; Kukaleva, N.; Li, G.; Wermter, H. *Macromol. Symp.* **2006**, *233*, 170–179. (d) Jain, S.; Bates, F. S. *Science* **2003**, *300*, 460–464.

(8) (a) Armstrong, G.; Buggy, M. *J. Mater. Sci.* **2005**, *40*, 547–559. (b) Brunsveld, L. B.; Folmer, J. B.; Meijer, E. W.; Sijbesma, R. P. *Chem. Rev.* **2001**, *101*, 4071–4097. (c) Bazzi, H. S.; Sleiman, H. F. *Macromolecules* **2002**, *35*, 9617–9620. (d) Ishihara, Y.; Bazzi, H. S.; Toader, V.; Godin, F.; Sleiman, H. F. *Chem.*−*Eur. J.* **2007**, *13*, 4560–4570.

(9) (a) Zhang, L.; Eisenberg, A. *Science* **1995**, *268*, 1728. (b) Zhang, L.; Eisenberg, A. *J. Am. Chem. Soc.* **1996**, *118*, 3168. (c) Zhang, L.; Yu, K.; Eisenberg, A. *Science* **1996**, *232*, 1777. (d) Jenekhe, S. A.; Chen, K. L. *Science* **1999**, *283*, 372.

(10) (a) Bucknall, D. G.; Anderson, H. L. *Science* **2003**, *302*, 1904–1905. (b) Mckee, M. G.; Layman, J. M.; Cashion, M. P.; Long, T. E. *Science* **2006**, *311*, 353–355. (c) Chen, W.-H.; Shao, X.-B.; Regen, S. L. *J. Am. Chem. Soc.* **2005**, *127*, 12727–12735.

(11) (a) Jenekhe, S. A.; Chen, X. L. *Science* **1998**, *279*, 1903–1907. (b) Chen, X. L.; Jenekhe, S. A. *Langmuir* **1999**, *15*, 8007.

(12) (a) Leininger, S.; Olenyuk, B.; Stang, P. J. *Chem. Rev.* **2000**, *100*, 853–908. (b) MacGillivray, L. R.; Atwood, J. L. *Nature (London)* **1997**, *389*, 469–472. (c) Prins, L. J.; Huskens, J.; de Jong, F.; Timmerman, P. D.; Reinhoudt, N. *Nature (London)* **1999**, *398*, 498–502. (d) Zhou, Y.; Antonietti, M. *J. Am. Chem. Soc.* **2003**, *125*, 14960–14961.

(13) (a) Fenniri, H.; Packiarajan, M.; Vidale, K. L.; Sherman, D. M.; Hallenga, K.; Wood, K. V.; Stowell, J. G. *J. Am. Chem. Soc.* **2001**, *123*, 3854–3855. (b) Hartgerink, J. D.; Beniash, E.; Stupp, S. I. *Science* **2001**, *294*, 1684–1688.

(14) (a) Stupp, S. I.; Son, S.; Lin, H. C.; Li, L. S. *Science* **1993**, *259*, 59–63. (b) Winfree, E.; Liu, F. R.; Wenzler, L. A.; Seeman, N. C. *Nature (London)* **1998**, *394*, 539–544. (c) Zepik, H.; Shavit, E.; Tang, M.; Jensen, T. R.; Kjaer, K.; Bolbach, G.; Leiserowitz, L.; Weissbuch, I.; Lahav, M. *Science* **2002**, *295*, 1266–1269. (d) Lin, Y.; Skaff, H.; Emrick, T.; Dinsmore, A. D.; Russell, T. P. *Science* **2003**, *299*, 226–229.

(15) (a) Martin, T.; Obst, U.; Rebek, J., Jr. *Science* **1998**, *281*, 1842–1845. (b) Hirschberg, J. H. K. K.; Brunsveld, L.; Ramzi, A.; Vekemans, J. A. J. M.; Sijbesma, R. P.; Meijer, E. W. *Nature (London)* **2000**, *407*, 167–170. (c) Boal, A. K.; Ilhan, F.; DeRouchey, J. E.; Thurn-Albrecht, T.; Russell, T. P.; Rotello, V. M. *Nature (London)* **2000**, *404*, 746–748.

(16) (a) Olenyuk, B.; Whiteford, J. A.; Fechtenkotter, A.; Stang, P. J. *Nature (London)* **1999**, *398*, 796–799. (b) Luo, S.; Liu, S.; Xu, J.; Liu, H.; Zhu, Z.; Jiang, M.; Wu, C. *Macromolecules* **2006**, *39*, 4517–4525. (c) Nie, Z.; Fava, D.; Kumacheva, E.; Zou, S.; Walker, G. C.; Rubinstein, M. *Nat. Mater.* **2007**, *6*, 609–614.

(17) (a) Zeng, X. B.; Ungar, G.; Liu, Y. S.; Percec, V.; Dulcey, S. E.; Hobbs, J. K. *Nature (London)* **2004**, *428*, 157–160. (b) Wang, Z. H.; Enkelmann, V.; Negri, F.; Mullen, K. *Angew. Chem., Int. Ed.* **2004**, *43*, 1972–1975. (c) Zubarev, E. R.; Sone, E. D.; Stupp, S. I. *Chem.*−*Eur. J.* **2006**, *12*, 7313–7327.

(18) (a) Velonia, K.; Rowan, A. E.; Nolte, R. J. M. *J. Am. Chem. Soc.* **2002**, *124*, 4224–4225. (b) Xu, J.; Zubarev, E. R. *Angew. Chem., Int. Ed.* **2004**, *43*, 5491–5496. (c) Pochan, D. J.; Chen, Z. Y.; Cui, H. G.; Hales, K.; Qi, K.; Wooley, K. L. *Science* **2004**, *306*, 94–97. (d) Hawker, C. J.; Wooley, K. L. *Science* **2005**, *309*, 1200–1205.

(19) Tung, P. H.; Kuo, S. W.; Chan, S. C.; Hsu, C. H.; Wang, C. F.; Chang, F. C. *Macromol. Chem. Phys.* **2007**, *208*, 1823–1831.

(20) (a) Jenekhe, S. A.; Alam, M. M.; Zhu, Y.; Jiang, S.; Shevade, A. *Adv. Mater.* **2007**, *19*, 536–542. (b) Otmakhova, O. A.; Kuptsov, S. A.; Talroze, R. V.; Patten, T. E. *Macromolecules* **2003**, *36*, 3432. (c) Cui, L.; Miao, J.; Zhu, L.; Sics, I.; Hasiao, B. S. *Macromolecules* **2005**, *38*, 3380–3388.

(21) (a) Deng, S.; Advincula, R. C. *Chem. Mater.* **2002**, *14*, 4073–4080. (b) Taranekar, P.; Fan, X.; Advincula, R. C. *Langmuir* **2002**, *18*, 7943–7952. (c) Xia, C.; Fan, X.; Park, M.; Advincula, R. C. *Langmuir* **2001**, *17*, 7893–7898. (d) Inaoka, S.; Advincula, R. C. *Macromolecules* **2002**, *35*, 1426–1428. (e) Park, M. K.; Xia, C.; Advincula, R. C.; Schutz, P.; Caruso, F. *Langmuir* **2001**, *17*, 7670–7677.

(22) (a) Lu, S.; Liu, T.; Ke, L.; Ma, D. G.; Chua, S. J.; Huang, W. *Macromolecules* **2005**, *38*, 8494–8502. (b) Zahn, S.; Swager, T. M. *Angew. Chem., Int. Ed.* **2002**, *41*, 4225–4230. (c) Lee, M.; Cho, B. K.; Zin, W. C. *Chem. Rev.* **2001**, *101*, 2869–3892.

(23) (a) Christiaan, E.; Steenwinckel, D. V.; Samyn, C. *J. Mater. Chem.* **2002**, *12*, 951–957. (b) Parada, J. M. R.; Percec, V. *Macromolecules* **1986**, *19*, 55–64. (c) Ho, M. S.; Barrett, C.; Paterson, J.; Esteghamatian, M.; Natansohn, A.; Rochon, P. *Macromolecules* **1996**, *29*, 4613–4618. (d) Ito, S.; Ohmori, S.; Yamamoto, M. *Macromolecules* **1992**, *25*, 185–191. (e) Ishizawa, H.; Nakano, T.; Yade, T.; Tsuji, M.; Nakagawa, O.; Yamaguchi, T. *J. Polym. Sci., Part A: Polym. Chem.* **2004**, *42*, 4656–4665. (f) Zhang, Y.; Wang, L.; Wada, T.; Sasabe, H. *Macromol. Chem. Phys.* **1996**, *197*, 667–6676. (g) Lowe, J.; Holdcroft, S. *Macromolecules* **1995**, *28*, 4608–4616. (h) Hallensleben, M.; Hollowdel, F.; Stanke, D. *Macromol. Chem. Phys.* **1995**, *196*, 3535–3547. (i) Jenekhe, S. A.; Osaheni, J. A. *Science* **1994**, *265*, 765–768.

(24) (a) Bonsei, S. M.; Erra-Balsells, R. *J. Lumin.* **2001**, *93*, 51. (b) Dotz, F.; Brand, J. B.; Ito, S.; Gherghel, L.; Mullen, K. *J. Am. Chem. Soc.* **2000**, *122*, 7707–7717. (c) Savariar, E. N.; Aathimanikandan, S. V.; Thayumanavan, S. *J. Am. Chem. Soc.* **2006**, *128* (50), 16224–16230. (d) Kim, B. S.; Hong, D. J.; Bae, J.; Lee, M. *J. Am. Chem. Soc.* **2005**, *127*, 16333–16337.

(25) (a) Yu, K.; Zhang, L.; Eisenberg, A. *Langmuir* **1996**, *12*, 5980–5984. (b) Choucair, A.; Eisenberg, A. *Eur. Phys. J. E* **2003**, *10*, 37–44. (c) Messmore, B. W.; Hulvat, E. D.; Stupp, S. I. *J. Am. Chem. Soc.* **2004**, *126*, 14452–14458. (d) Vaghese, R.; S Gerge, J.; Ajayaghosh, A. *Chem. Commun.* **2005**, *59*, 3–595.

(26) (a) Balakrishnan, K.; Datar, A.; Zhang, W.; Moore, J. S.; Zang, L. *J. Am. Chem. Soc.* **2006**, *128*, 6576–6577. (b) Weck, M.; Dunn, A. R.; Matsunoto, K.; Coates, G. W.; Lobkovsky, E. B.; Grubbs, R. H. *Angew. Chem., Int. Ed.* **1999**, *38*, 2741–2745. (c) Alexander, L. E. *X-Ray Diffraction Methods in Polymer Science*; John Wiley & Sons: New York, 1969.

(27) (a) Lyuksyutov, S. F.; Sancaktar, E. *Nat. Mater.* **2003**, *2*, 468–472. (b) Dubois, J. E.; Desbene, M. A.; Lacaze, P. C. *J. Electroanal. Chem.* **1982**, *132*, 177. (c) Jagadesan, S.; Sindhu, S.; Advincula, R. C.; Valiyaveettil, S. *Langmuir* **2006**, *22*, 780–786. (d) Jegadesan, S.; Sindhu, S.; Valiyaveettil, S. *Small* **2006**, *2*, 481–484. (e) Jagedesan, S.; Tranekar, P.; Sindhu, S.; Advinclula, R. C.; Valiyaveettil, S. *Langmuir* **2006**, *22*, 3807–3811.

(28) (a) Hilger, A.; Gisselbrecht, J. P.; Tykwinski, R.; Boudon, C.; Schrieber, M.; Martin, R.; Luthi, H.; Gross, M.; Diederich, F. *J. Am. Chem. Soc.* **1997**, *119*, 2069. (b) Romero, D.; Nuesch, F.; Benazzi, T.; Ades, D.; Siove, A.; Zuppiroli, L. *Adv. Mater.* **1997**, *9*, 1158. (c) Ambrose, J.; Carpenter, L.; Nelson, R. *J. Electrochem. Soc.* **1975**, *122*, 876. (d) Xia, C.; Advincula, R. C.; Baba, A.; Knoll, W. *Chem. Mater.* **2004**, *16*, 2852–2856.

(29) (a) Mccullough, R. D.; Ewbank, P. C.; Loewe, R. S. *J. Am. Chem. Soc.* **1997**, *119*, 633–634. (b) Morin, J. F.; Leclerc, M. *Macromolecules* **2002**, *35*, 8413–8417. (c) Ballav, N.; Biswas, M. *Synth. Met.* **2003**, *132*, 213–218. (d) Kumpumbu, K. L.; Leclerc, M. *Chem. Commun.* **2000**, *19*, 1847–1848. (e) Ho, H. A.; Boissinot, M.; Bergeron, M. G.; Corbeil, G.; Dore, K.; Boufreau, D.; Laclerc, M. *Angew. Chem., Int. Ed.* **2002**, *41*, 1548–1551.

(30) (a) Li, Y.; Ding, J.; Day, M.; Tao, Y.; Lu, J.; D'iorio, M. *Chem. Mater.* **2004**, *16*, 2165–2173. (b) Ahn, T.; Song, S, Y.; Shim, H.-K. *Macromolecules* **2000**, *33*, 6764–6771. (c) Briere, J.-F.; Cote, M. *J. Phys. Chem. B* **2004**, *108*, 3123–3129. (d) Thomas, K. R. J.; Lin, J. T.; Lin, Y.-Y.; Tsai, C.; Sun, S.-S. *Organometallics* **2001**, *20*, 2262–2269.

(31) (a) Guay, J.; Paynter, R.; Dao, L. H. *Macromolecules* **1990**, *23*, 3598–3605. (b) Kemp, W. *Organic Spectroscopy*; Palgrave: New York, 1991. (c) Pavia, D. L.; Lampman, G. M.; Kriz, G. S. *Introduction to Spectroscopy: A Guide for Students of Organic Chemistry*; Saunders: Philadelpha, 1979.

(32) (a) Abe, Y.; Bernede, J.; Delvale, A. M.; Tregouet, Y.; Diaz, R.; Lefrrant, S. *Synth. Met.* **2002**, *126*, 1–6. (b) Xia, C.; Advincula, R. C.; Baba, A.; Knoll, W. *Chem. Mater.* **2004**, *16*, 2852–2856. (c) Xia, C.; Fan, X.; Park, M.; Advincula, R. C. *Langmuir* **2001**, *17*, 7893–7898. (d) Zotti, G.; Zecchin, S.; Berlin, A.; Schiavon, G.; Giro, G. *Chem. Mater.* **2001**, *13*, 43. (e) Zotti, G.; Schiavon, G.; Zecchin, S.; Morin, J. F.; Leclerc, M. *Macromolecules* **2002**, *35*, 2122–2128.

MA8008349